Chemical and Process Engineering: New Frontiers, 2025, 46(2), e91
DOI: 10.24425/cpe.2025.153676

CRITICAL REVIEW

Current trends in the application of CFD and Artificial Intelligence to simulate the behavior of respiratory and circulatory systems

Krystian Jędrzejczak[1], Bogdan Ciszek[2], Malenka M. Bissell[3], Wojciech Orciuch[1], Łukasz Makowski[1]*

[1] Warsaw University of Technology, Faculty of Chemical and Process Engineering, Waryńskiego 1, Warsaw, Poland
[2] Medical University of Warsaw, Center of Biostructure, Departament of Descriptive and Clinical Anatomy, Warsaw, Poland
[3] University of Leeds, Leeds Institute of Cardiovascular and Metabolic Medicine, Leeds, UK

* **Corresponding author, e-mail:** lukasz.makowski.ichip@pw.edu.pl

Chemical Engineering Horizons and Perspectives. Article series endorsed by the Scientific Committee on Chemical and Process Engineering of the Polish Academy of Sciences, term 2024–2027.

Article info:
Received: 30 April 2025
Revised: 15 May 2025
Accepted: 26 May 2025

Abstract

Background: In the 21st century, respiratory and cardiovascular diseases have become increasingly prevalent, posing significant challenges for healthcare systems. The growing incidence of these conditions has driven the adoption of advanced technologies, such as computer simulations and artificial intelligence (AI), to improve diagnostic accuracy and optimize treatment strategies. *Methods:* Mathematical equations used in chemical engineering to describe fluid dynamics can be adapted to model airflow in the respiratory system and blood flow in the circulatory system. Computational fluid dynamics (CFD) simulations, combined with modern medical imaging techniques, allow for the development of detailed 3D models of anatomical structures, enabling precise assessments of physiological functions. *Results:* The integration of AI and CFD models has significantly enhanced disease diagnosis and treatment planning. AI-driven algorithms facilitate automated image analysis, predictive modeling and real-time decision support, leading to improved patient outcomes. These technologies allow for early detection of abnormalities, personalized treatment approaches, and better risk assessment in clinical practice. *Conclusions:* Close collaboration between engineers and physicians is revolutionizing the medical field, opening new possibilities for diagnosing and managing respiratory and cardiovascular diseases. The continuous advancement of AI and computational modelling is transforming medicine, making healthcare more precise and efficient. Future research should focus on refining these technologies, ensuring their seamless integration into clinical practice to further enhance patient care.

Keywords
respiratory system, circulatory system, computational fluid dynamics, artificial intelligence, medical imaging

1. INTRODUCTION

21st century lifestyle changes which increasing rates of obesity and deteriorating air quality caused by environmental degradation have contributed to noticeable increase in the prevalence of cardiovascular and respiratory diseases. These adverse trends have resulted in a growing demand for innovative diagnostic methods and more effective treatment options for these conditions. Over the past several decades, the application of numerical methods in modeling human physiology has seen significant growth. Technologies such as artificial intelligence (AI) and computational fluid dynamics (CFD) software enable a deeper understanding of the mechanisms that govern the functioning of the human body. These tools make it possible to analyze complex biological processes with unprecedented precision, such as blood flow within the cardiovascular system or gas exchange in the lungs. The integration of AI and CFD offers a synergistic approach that enhances the efficiency and accuracy of analyses. For instance, neural network models can be trained using precise solutions derived from CFD simulations, enabling AI to rapidly predict the behavior of biological systems. This capability is particularly valuable for advancing personalized medicine, where diagnostic and therapeutic strategies can be tailored to the unique physiological characteristics of individual patients.

The progress in computational analysis has been enhanced by parallel advancements in medical diagnostic methods. Modern imaging technologies, such as computed tomography (CT) and magnetic resonance imaging (MRI), provide detailed information about the geometry of anatomical structures and offer insights into dynamic parameters such as blood flow patterns. These complementary data sources are essential for creating realistic and accurate numerical models. A groundbreaking diagnostic technique that has emerged in recent years is 4D Flow MRI. This advanced imaging method allows for the simultaneous acquisition of both anatomical and flow-related data

in real-time. It has significant potential in the diagnosis and management of cardiovascular diseases, offering a comprehensive assessment of the dynamic processes occurring within the circulatory system. The potential of 4D Flow MRI becomes even more apparent when combined with CFD modeling and artificial intelligence. By integrating these technologies, researchers and clinicians can achieve a higher level of precision in simulating biological processes. For example, data obtained from 4D Flow MRI can be used to validate CFD models, which in turn can enhance the accuracy of AI-driven predictions. This integrated approach enables the simulation of complex scenarios, such as the impact of vascular abnormalities or the hemodynamic consequences of surgical interventions. Thus, the combination of modern diagnostic techniques like 4D Flow MRI with computational tools opens up new possibilities for improving patient care. Despite its promise, the integration of 4D Flow MRI, CFD, and AI faces several challenges: high computational demands, the need for robust algorithms and the availability of quality training data are key factors that must be addressed. Additionally, interdisciplinary collaboration between engineers, clinicians, and data scientists is essential to ensure that these technologies meet the needs of medical practice. The convergence of advanced diagnostic imaging, computational fluid dynamics and artificial intelligence represents a transformative leap in the field of medicine. This interdisciplinary approach holds immense potential to improve the quality of healthcare by enabling more accurate diagnoses, better treatment planning, and deeper insights into the complexities of human physiology. As these technologies continue to evolve and integrate, they promise to play a pivotal role in addressing the growing burden of cardiovascular and respiratory diseases in the modern world. This literature review seeks to explore the multifaceted contributions of chemical engineering to the rapidly evolving field of personalized medicine. Central to this exploration is the application of computational fluid dynamics, a powerful tool traditionally employed in engineering disciplines, which is now being adapted to model complex physiological processes within the human body. By integrating CFD with advanced diagnostic technologies and artificial intelligence, researchers aim to revolutionize patient care through highly individualized therapeutic strategies.

2. ANATOMY OF SELECTED SYSTEMS OF HUMAN BODY

The phenomenon of flow is observed in several systems of human body. This is circulatory system (blood), lymphatic system – lymph, respiratory apparatus – air and central nervous system – cerebrospinal fluid. Of course the flow of organic fluids or gases is observed in other systems an organs such as glands of external secretion: liver, pancreas or salivary glands and others, urinary system, alimentary tract but the flow in these systems is more or less periodical. The first four present continuous flow.

2.1. Respiratory system

The respiratory system is composed of air ways: nose, pharynx, larynx and trachea which bifurcate on two main bronchi which enter to the lungs. The bronchial tree hierarchically divides into lobar, segmental and lesser elements. These conduct air through the alveolar ducts to the pulmonary acinus partly divided in several alveolar sacs which are composed of alveoli. During inspiration the air flows to the alveoli and during expiration in reverse. However, alveoli do not collapse but retain some air. The process of inspiration/expiration – ventilation of the lungs is supported by the structure of the thorax. The thoracic cage is composed of 12 pairs of ribs which run from vertebral column to the sternum. The intercostal spaces are filled with intercostal muscles. The inlet of the thorax is closed by diaphragm muscle. On the external surface of the thorax additional muscles are attached for control of respiratory movements. The process of inspiration lowers the intrathoracic pressure by enlarging of thoracic cage cavity: Vertical diameter also increases by lowering the diaphragm when it contracts. External intercostal and some additional superficial muscle elevate ribs leading to enlargement of the transverse and sagittal diameter. Expiration is the reverse process but passive: the thorax collapses under its own weight and the weight of elastic fibers of in the lungs tissue. In case of fibrosis of lungs or obturation of airways, some additional force is needed which is developed by expiratory muscles. The shape of the nasal cavity is very complex due to turbinates which enter the lumen and the septum dividing nasal cavity into left and right side. The air flow through the nose may by disturbed by mucosal edema and secretion of nasal glands and paranasal sinuses. The pharynx is a vertical cavity which collapses during swallowing (see Fig. 2). The larynx also plays an important role in phonation. Therefore the shape of its cavity is modified by a number of mobile folds. From this moment trachea and bronchi are simple tubes (see Fig. 3). The 3/4 of its wall is composed of horseshoe like cartilage and posterior wall is membranous. In the wall there are smooth muscles which control the diameter of bronchi under the control of the vagus nerve. During physiological respiration with inspiration bronchi enlarge and with expiration slightly narrow and elevate pressure in the airways thus protecting alveoli from collapse. Constriction of bronchi during asthma and other obturation disorders makes expiration difficult. The lumen of bronchi may be also reduced by edema of mucosa and secretion of bronchial glands as well as pathological fluids produced during inflammatory status. The ventilation of lungs

maintains high partial pressure of oxygen in the alveoli and very low pressure of CO_2. The diffusion gradient between alveoli and blood inflowing from pulmonary trunk (low oxygen high CO_2 – venous blood) is a base of gas exchange. In the capillary network of alveoli venous blood transforms into arterial blood (high oxygen low CO_2) (Ghafarian et al., 2016; Ninke et al., 2024; Patwa and Shah, 2015).

2.2. Circulatory and lymphatic systems

2.2.1. Circulatory system

The two main parts of the circulatory system are the heart and blood vessels. The lumen of the circulatory system is filled with blood. The human (mammalian) circulatory system is closed – blood does not exit the lumen. The heart plays the role of a muscular pump which gives kinetic energy to the blood. The heart is composed of four chambers: two atria and two ventricles. Arteries are vessels which conduct blood away from the heart. Veins conduct blood back to the heart chambers. The walls of vessels are composed of three layers. The innermost is the tunica intima, composed of one layer of endothelial cells based on subendothelial smooth muscle cells and an internal elastic lamina. Next is the tunica media, which is much thicker and contains many elastic fibers or many smooth muscle cells supported by an external elastic membrane. The last layer, the tunica adventitia, is composed mainly of collagen fibers. The tunica media of arteries is much thicker than that of veins. So arteries do not collapse and are resistant to internal blood pressure (Piechna et al., 2017), while veins have thin walls and are easy to compress.

Venous blood returns from the body through the inferior and superior vena cava to the right atrium. From the right atrium, blood flows through the right atrioventricular (tricuspid) valve to fill the right ventricle until the valve closes. This protects the blood from flowing backward. The ventricle contracts and blood is pumped through the pulmonary valve to the pulmonary trunk. When the pressure in the ventricle decreases, backflow closes the pulmonary valve. The blood flows to the lungs through branches of the pulmonary arteries to the level of the capillary network of the alveoli, where gas exchange occurs. Then oxygenated blood flows through the pulmonary veins to the left atrium (Polaczek et al., 2019). From the left atrium, blood passes through the left atrioventricular (bicuspid or mitral) valve into the left ventricle. Similarly to the right side, after filling, the mitral valve closes and the contraction of the ventricle ejects the blood through the aortic valve into the aorta, which closes, like the pulmonary valve, after ejection. The chambers of the heart are divided by the interatrial and interventricular septa, so venous and arterial blood do not mix. The described processes – valve closing and ventricular contraction – are executed simultaneously on the right and left sides of the heart. Because the pulmonary circulation constitutes low resistance and the resistance of the systemic circulation is much greater, the pressure developed by the left ventricle should be about 6 times greater than that in the right ventricle. So the muscle wall of the left ventricle is much greater than that of the right.

Branches of the aorta divide hierarchically at the beginning. Later, they are organized into a network. The diameter of arteries decreases up to the level of the capillary network of tissues and organs. In this region, reverse gas exchange is observed: tissues take oxygen for metabolism and produce CO_2. Thus arterial blood is transformed into venous blood.

The flow through veins is supported by the small pressure from the capillary network, the sucking effect of the right side of the heart and pressure changes due to respiratory movements of the thorax. In the limbs, a system of venous valves and periodic compression from skeletal muscles protect against backflow. Through the venous network and main venous trunks, blood flows to the superior and inferior vena cava. The cycle of circulation is closed (Cieślicki et al., 2002; Standring et al., 2005). The work of the circulatory system is oscillatory due to the cycle of the heart: systole (contraction and ejection) and diastole, when the pressure should drop. The heart cycle is controlled by its own autonomic conduction system. It generates and distributes bioelectrical stimuli (action potentials) in the myocardium. The autonomic nervous system modulates this action. The sympathetic nervous system increases heart rate and blood pressure, while the parasympathetic (vagus) decreases both values (Standring et al., 2005).

Many organs (brain, kidneys) need continuous flow. The aorta and its big branches have a thick tunica media rich in elastic fibers. During the ejection of blood from the left ventricle (systole), they act as a "ballon," storing energy in the stretched wall. During diastole, the contracting wall supports blood pressure in the arterial system. More distal arteries are of the muscular type. Their smooth muscle tunica media is innervated by autonomic fibers. It is also controlled by the level of respiratory gases (oxygen narrows arteries, while CO_2 enlarges them due to the relaxation of smooth muscles).

Many biochemical agents, metabolites and hormones influence the tunica media tension. This is a source of different regional flows in different pathophysiological states. For example, during physical effort, due to fight or escape, arteries to the skeletal muscle enlarge, while arteries to the digestive tract contract. Heart rate and blood pressure increase. This is under the influence of sympathetic fibers and the ejection of catecholamines from the adrenal glands (Syed et al., 2023). A detailed model of the circulatory system is presented in Fig. 1.

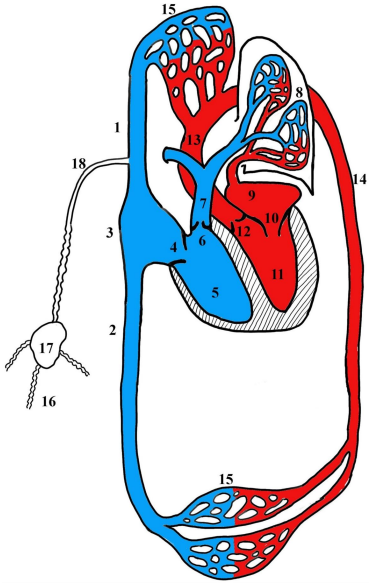

Figure 1. Scheme of circulatory system; blue – deoxygenated – "venous" blood red – oxygenated – "arterial" blood. 1. superior vena cava, 2. inferior vena cava, 3. right atrium, 4. tricuspidal valve, 5. right ventricle, 6. pulmonary valve, 7. pulmonary trunk, 8. pulmonary capillary network, 9. left atrium, 10. mitral valve, 11. left ventricle, 12. aortic valve, 13. aorta arch, 14. aorta continuation, 15. systemic capillary network, 16. lymphatic vessels, 17. lymphonode, 18. thoracic duct – main lymphatic vessel entering venous system.

2.2.2. Pathophysiology of circulatory system and modeling

Disturbances in blood flow may be related to dysfunction of the heart or blood vessels. One of the very frequent and dangerous pathologies is the formation of atherosclerotic plaque in the wall of a vessel – mainly arteries. The plaque is located in the tunica media, under the intima, and is a collection of cholesterol-derived substances. The growing plaque decreases the diameter of the artery. Critical narrowing is from 80 to 90% of the cross-section covered by the plaque. It is a source of signs of ischemia in the heart (angina pectoris), brain, kidneys, limbs, and other regions. When the intima is removed, even a small plaque may be a site of aggregation of thrombocytes (cells responsible for one of the clotting mechanisms in the blood). Such a thrombus may propagate with the blood stream, closing distal vessels as an embolus. This is one of the most frequent mechanisms of ischemic stroke. When the lumen of an artery is small (2–3 mm in diameter), exposure of the plaque provokes a thrombus which closes the artery at once. It is a very frequent mechanism of heart infarction (see Fig. 6). The formation of atherosclerotic plaque is related to uncontrolled hypertension, metabolic disturbances like dyslipidemia, diabetes, unhealthy habits: smoking, high-fat consumption and genetically based diseases. The location of plaques is characteristic for branching sites due to shear stress (see below). If the closed artery is the only source of blood supply to the desired region (an end artery, anatomically or physiologically), necrosis develops from 3–4 minutes for the brain to 6 hours for the heart and skeletal muscle and 12 hours for connective tissue and bones. When the closed artery is part of a network with the possibility of collateral circulation, the incident may be even asymptomatic or cause chronic or repetitive dysfunction (Tomaszewski et al., 2024).

Malformations of the vessel wall – aneurysm: saccular (mainly in the brain) and fusiform (mainly atherosclerotic aorta) when ruptured are a source of bleeding, frequently lethal. Disturbances of flow in the aneurysmal dome are a source of shear stress and provoke wall degeneration, which leads to rupture due to the loss of resistance to intravascular pressure. Because the moment of rupture is difficult to predict, modeling of flow and vessel wall gives hope for a solution to this problem (Ciszek et al., 2013; Rzepliński et al., 2025).

In the venous system, modeling of flow is extremely difficult due to an unstable diameter (the effect of external pressure on the wall) and generally a network-like organization almost up to the level of the heart. The most frequent venous pathology in the limbs: varicose veins, constitutes an enlarged network, partly closed by thrombi which can be recanalized. Heart disturbances influence flow in two main ways. Insufficiency causing ischemia of organs. It is due to valve defects, or partial loss of contractility due to infarcts, myocardium diseases, or heart rate disturbances – arrhythmia. This last, like atrial fibrillation, may be a source of emboli which can propagate to the pulmonary or systemic circulation. Thrombi from veins of the lower extremity (see above) may propagate to the pulmonary arteries via the chambers of the right side of the heart and be a source of sudden death. In the case of a congenital defect: patent foramen ovale in the interatrial septum, released thrombi from the veins of the lower limbs may reach the left atrium and systemic circulation, occluding various arteries (Standring et al., 2005).

2.2.3. Lymphatic system

This system starts as a network of narrow blind vessels which drain fluids from the intercellular space. Lymph flows through lymph nodes which play an immunological role. The vessels are supplied with numerous valves. Contractility of lymphatic vessels is one of the sources of flow. Others are changes in local tissue pressure during movements, pulsatility of nearby arterial trunks, and pressure changes in the thorax during respiration. Finally, through the thoracic duct and the right lymphatic duct, lymph flows out to the veins close to the heart. So the suction effect of the heart also supports flow in these vessels. Disturbances of flow in the lymphatic system are observed after oncologic resections when nodes are removed as sites of metastases or due to blockage of vessels by parasites. The effect is edema or limb elephantiasis: a monstrous enlargement of a limb (Jankowska-Steifer et al., 2021; Ratajska et al., 2014).

2.3. Central nervous system

Cerebrospinal fluid is produced in the ventricular system of the brain by the choroid plexus. Up to 500 ml / 24 h is produced. It is about 0.3 ml /min. The ventricular system has a very complicated shape and the only tubular structure is the cerebral aqueduct which is 2 mm in diameter and 10 mm at its longest. The flow observed here is two-way. Cerebrospinal fluid flows out to the subarachnoid space which covers the surface of the central nervous system, so its shape is the most complicated of all spaces in the human body. Finally, it is resorbed into the venous and lymphatic system. The main disturbance is observed when flow is stopped in the ventricular system and a collection of fluid forms before the site of obstruction, causing enlargement of ventricles – hydrocephalus. The same effect is observed when resorption into the venous system is impaired (Ciołkowski et al., 2011; Skadorwa et al., 2010).

3. NUMERICAL METHODS IN MEDICINE

Numerical methods in medicine are increasingly being used to describe physical phenomena occurring in the human body. The development of modern information technologies enables not only a reduction in computation time but also the advancement of personalized models tailored to individual patients. In recent years, there has been a visible trend of shifting from CPU-based computations to GPU-based computations (Viola et al., 2023). This trend is particularly evident in artificial intelligence computations, which are evolving dynamically alongside advancements in successive generations of graphics cards. For computational fluid dynamics, this transition is also noticeable, although the pace of change is slower. This is due to the lower efficiency of GPUs in double-precision computations, which are often required in CFD. Furthermore, the relatively nascent support for CFD computations on GPUs means that CPUs currently maintain an edge in terms of functionality and performance. However, in the next decade, significant progress is expected in the domain of CFD computations using modern GPUs. This anticipated growth is driven by continuous improvements in GPU architecture, enhanced support for double-precision arithmetic, and increasing adoption of GPU-accelerated libraries and frameworks specifically designed for CFD tasks. As these technologies mature, GPUs could surpass CPUs in performance and functionality for CFD, potentially revolutionizing the field by enabling faster simulations, real-time analysis, and broader accessibility to advanced computational techniques. This shift could also open new possibilities for real-time applications, such as patient-specific simulations and predictive modeling in medicine, further bridging the gap between computational advancements and clinical practice.

In CFD simulations of both the respiratory and cardiovascular systems, the accuracy of geometry segmentation and the definition of appropriate boundary conditions are critically important. Human-based segmentation involves many pitfalls, particularly inconsistencies in evaluating the boundaries between individuals. These inconsistencies arise from differences in visual analysis and decision-making processes in the brain, such as determining where measurements should start and end. Additionally, physical differences in using input devices, such as mice or trackballs, may influence the segmentation process. The quality of segmentation largely depends on the quality of the raw imaging data, which varies depending on the imaging modality. While the basic segmentation process typically involves selecting an appropriate intensity threshold in DICOM file analysis software, more advanced algorithms are also available. For instance, the Grow from Seeds method, implemented in open-source platforms such as 3D Slicer, offers improved segmentation capabilities. In commercial software, artificial intelligence algorithms are increasingly being employed to enhance the segmentation of vessels and other anatomical structures. Regarding boundary conditions, the selection of appropriate flow parameters often relies on experimental measurements obtained through Doppler ultrasound techniques or 4D Flow MRI. To further implement boundary conditions, simplified models – such as the three-element Windkessel model – are frequently used to replicate the pulsatile nature of blood flow (Kim et al., 2010; Luisi et al., 2024).

3.1. CFD simulations of the respiratory system

Modeling the respiratory system using computational fluid dynamics allows the study of airflow and the factors that affect it. It is used to analyze both normal breathing and cases involving diseases or structural issues in the respiratory system (Hu et al., 2023). Figure 2 illustrates the analysis of wall shear stress using CFD as a function of mouth opening during breathing (Hu et al., 2023).

An important aspect of this modeling is the division of the respiratory system into upper and lower airways, which differ in structure and airflow characteristics. The upper airways, including the nose, nasal cavity, pharynx and larynx, have a complex structure with narrow passages and sharp turns, leading to turbulent airflow. They are responsible for filtering, humidifying, and warming the air. CFD modeling is useful for studying nasal resistance, which may be caused by conditions such as a deviated septum or nasal polyps (Nishijima et al., 2018). It also helps in planning surgeries such as septum correction (Burgos et al., 2024; Na et al., 2022; Ormiskangas et al., 2022) and in analyzing conditions such as sleep apnea (Jeong et al., 2007; Mylavarapu et al., 2009, 2013), where airflow in the throat is blocked during sleep. The lower airways, including the trachea, bronchi, bronchioles, and alveoli, form a branching structure that becomes narrower as it goes deeper into the lungs (Shang et al., 2019). In the larger airways, airflow is often turbulent, while in the smaller airways, it transitions to smooth laminar flow, allowing for effective gas exchange in the alveoli. CFD modeling of the lower airways enables the analysis of airflow distribution, particularly in

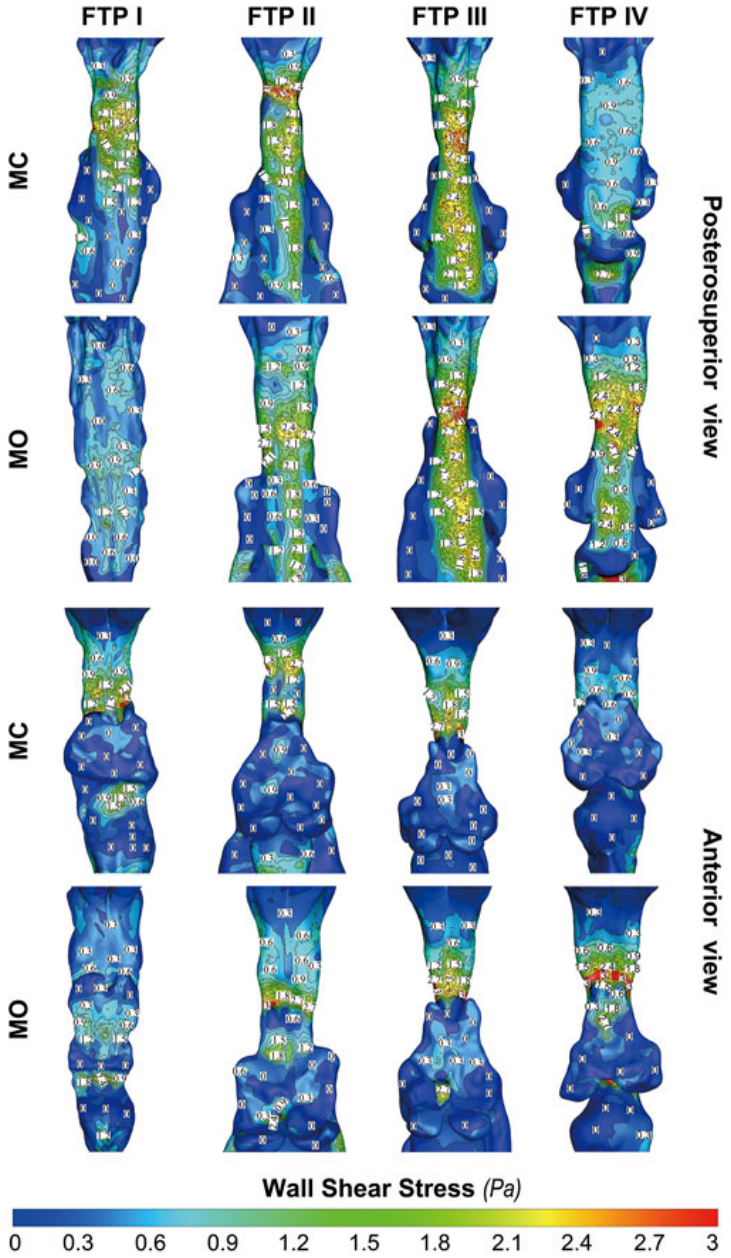

Figure 2. The contour of wall shear on the pharyngeal wall. Note, MC, mouth closed position; MO, mouth opening position; FTP, Friedman Tongue Position (Hu et al., 2023). Copyright © 2023 Hu B., Yin G., Fu S., Zhang B., Shang Y., Zhang Y., Ye J. Licensed under CC BY 4.0.

diseases such as asthma (De Backer et al., 2008) or chronic obstructive pulmonary disease (COPD) (Paz et al., 2017) and after surgical procedures such as pulmonary lobectomy (Aliboni et al., 2022; Tullio et al., 2021), as shown in Fig. 3.

It also allows the simulation of drug delivery, such as how inhalers distribute medication in the lungs (Kuprat et al., 2021; Sadafi et al., 2024; Xi et al., 2015; Xu et al., 2017), and the study of airway shape changes during breathing (Pirnar et al., 2015), which is important in diseases such as pulmonary fibrosis (Na et al., 2022). Modeling the respiratory system in healthy individuals helps to understand how efficiently the lungs function during different activities, such as physical exertion or in polluted environments. It also provides insights into how factors like age or altitude affect breathing (Tsega, 2018). In cases of illness, CFD helps detect blockages in the airways caused by tumors or foreign bodies (Bao et al., 2022; Hudson et al., 2023; Zobaer and Sutradhar, 2021). It also improves medical devices such as stents, inhalers, or CPAP machines and predicts the progression of diseases, helping to understand how changes in the respiratory system affect breathing. Although numerical modeling plays an important role in medical research and device development, experimental verification is required to ensure its validity and accuracy. This can be achieved either by clinical trials or by utilizing physical phantoms (Schewe et al., 2012), which may be realistic or

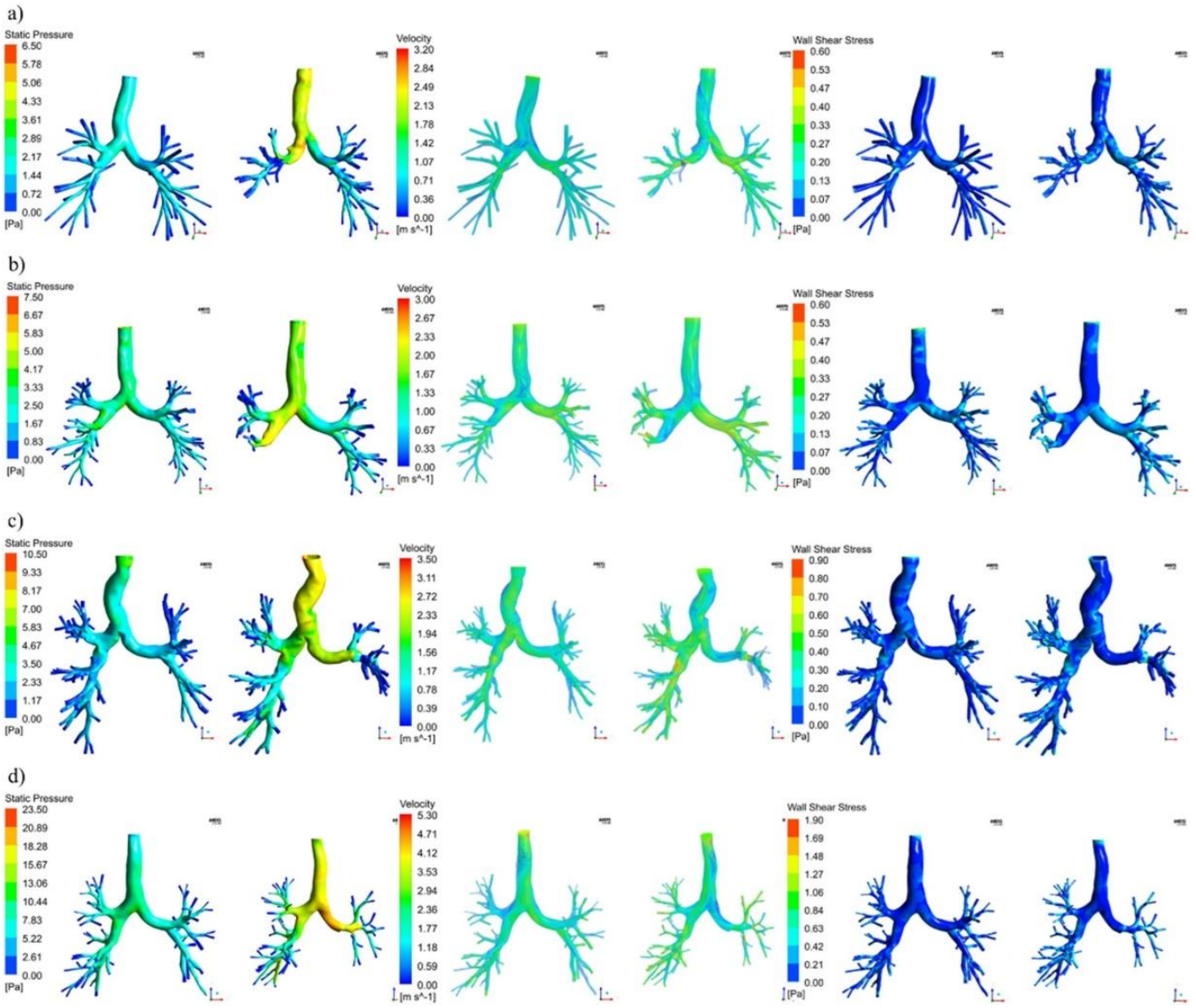

Figure 3. Contours of wall pressure (left), velocity streamlines (middle), contours of wall shear stress (right) on the global models for four representative subjects. (a) subject 2, right upper pulmonary lobectomy; (b) subject 6, right lower pulmonary lobectomy; (c) subject 9, left upper pulmonary lobectomy; (d) subject 12, left lower pulmonary lobectomy (Fluent v16, CFD-Post v16-Ansys, www.ansys.com) (Aliboni et al., 2022).

simplified. These phantoms provide a controlled environment for testing hypotheses and refining computational models. For measurements performed with medical equipment, magnetic resonance imaging (MRI) is a valuable tool (Han et al., 2023). Beyond its conventional diagnostic capabilities, MRI techniques can be leveraged to capture flow velocity data, offering insights into the dynamics of air movement in the respiratory tract. However, conducting experimental studies with hospital-grade equipment may not always be feasible due to cost, logistical challenges, or the specific requirements of the research. In such cases, advanced laser-based techniques, like Particle Image Velocimetry (PIV), provide a powerful alternative. PIV enables precise, high-resolution visualization and measurement of flow dynamics (Phuong and Ito, 2015; Sul et al., 2018). When combined with 3D-printed phantoms (Collier et al., 2018) that replicate the physiological geometry of anatomical structures, such as sections of the respiratory system, this method becomes even more effective. These phantoms can be customized to mimic specific patient anatomies or pathological conditions, making them invaluable for research, device testing, and the optimization of treatment strategies. Once CFD models are experimentally validated, they can serve as powerful tools in medical applications, particularly in the diagnosis and treatment planning of respiratory system conditions (Akor et al., 2024; Gamrot-Wrzołet al., 2020). These models provide detailed insights into the airflow dynamics, pressure distributions and particle transport within the respiratory tract, enabling clinicians to better understand patient-specific conditions.

3.2. CFD simulations of the circulatory system

Computational fluid dynamics is a powerful tool for analyzing blood flow within the circulatory system and the heart (Arminio et al., 2024; Białecki et al., 2024; Chiastra et al., 2023; Dedč et al., 2021; Ekmejian et al., 2024; Shiina et al., 2024). It enables researchers and clinicians to explore how blood moves through the body under various conditions, both during rest and physical activity. This makes it possible to gain insights into the functioning of healthy individuals as well as those with a wide range of cardiovascular conditions. CFD is particularly valuable for its ability to model the human body at different stages of life, from the earliest phases of fetal development through fetal life (Kasiteropoulou et al., 2020; Salman et al., 2021), childhood (Ait Ali et al., 2024; Hoganson et al., 2024; Malec et al., 2017) to adulthood (Jędrzejczak et al., 2024a; Kozłowski et al., 2021, 2022; Wojtas et al., 2021). In the early stages of life, congenital heart defects and vascular abnormalities are a major area of concern (Pennati et al., 2013). These conditions, such as hypoplastic aortic arch or aortic coarctation, can significantly impact blood flow and oxygen delivery throughout the body. Using CFD, engineers can create patient-specific models based on imaging data, such as MRI or CT scans, to simulate how blood flows through these malformed structures. This allows for a detailed understanding of how the abnormalities affect the heart and circulatory system and provides critical information for planning surgical corrections or other interventions. By accurately predicting the outcomes of potential treatments, CFD helps improve the success rates of procedures and reduce risks for young patients. As individuals age, the focus shifts from congenital issues to acquired conditions, such as atherosclerosis (Ahadi et al., 2024; Chaichana et al., 2012; Chen et al., 2017, 2020, 2024; Conijn and Krings, 2022; De Nisco et al., 2021; Jędrzejczak et al., 2023a, 2023b, 2023c, 2024a; Milewski et al., 2024; Morbiducci et al., 2020; Song et al., 2000; Yang et al., 2025), hypertension (Gao et al., 2025; Jędrzejczak et al., 2024b; Zuo et al., 2022), and the complications they cause, like aneurysms (Boite et al., 2023; Chiu et al., 2018; Jansen et al., 2014; Jayendiran et al., 2018; Li et al., 2020; Wang and Li, 2011) or strokes (Luisi et al., 2024; Rahma et al., 2022). CFD is particularly effective in studying these diseases because it can simulate how blood interacts with the walls of arteries and veins, including areas of narrowing, plaque buildup or weakened vascular walls. For example, in the case of atherosclerosis, CFD can help predict how a narrowing artery affects wall shear stresses, blood pressure, and flow patterns, which is crucial for understanding the progression of the disease and for planning interventions such as stent placement. CFD allows for the analysis of pathological changes across an entire cohort to examine how a given condition affects hemodynamic changes. Similarly, in hypertension, CFD models can reveal how elevated blood pressure impacts the vascular system over time, leading to better strategies for managing the condition. The literature contains numerous reports on the application of computational fluid dynamics (CFD) in analyzing various types of hypertension. Figure 4 illustrates one such application, where CFD is used to compare the hemodynamic differences between central and peripheral chronic thromboembolic pulmonary hypertension (CTEPH) (Tsubata et al., 2023).

The circulatory system is incredibly complex, comprising a vast network of vessels ranging from large arteries, like the aorta, to smaller arterioles and capillaries. Each type of blood vessel has unique dimensions, structures, and flow characteristics, making the study of blood flow dynamics a rich and challenging area of research. CFD allows for detailed modeling of these diverse components, providing insights into how blood moves through different parts of the body under varying physiological conditions. For example, researchers can simulate how blood flow changes during exercise, stress or the progression of disease. This is not only valuable for understanding how the circulatory system functions but also for designing medical devices, such as artificial heart valves, stents, and vascular grafts, tailored to specific patient needs. Another advantage of CFD is its ability to simulate scenarios that would be difficult or impossible to study experimentally. For instance, CFD can be used to investigate blood flow patterns in rare or extreme conditions, such as during aortic dissection (Karmonik et al., 2013; Zhu et al., 2022, 2023) or after a complex surgical procedure. Figure 5 illustrates the application of CFD in modeling aortic dissection, along with the capability to monitor disease progression (Zhu et al., 2022).

This capability extends the range of what is possible in cardiovascular research and provides a non-invasive way to explore new diagnostic techniques or therapeutic approaches. Numerical modeling of the circulatory system, similar to the modeling of the respiratory system, requires appropriate experimental verification. For this purpose, Particle Image Velocimetry (PIV) measurements can be utilized, leveraging 3D-printed phantoms of the circulatory system to replicate complex blood flow dynamics in controlled environments (Antonowicz et al., 2023; Ho et al., 2020; Jędrzejczak et al., 2023a; Li et al., 2020; Park et al., 2016; Saaid et al., 2019). These phantoms enable the validation of computational models by providing high-resolution experimental data on flow patterns, velocities, and turbulence. In clinical settings, several advanced techniques are available to support the verification process. Doppler-based apparatus, such as Doppler ultrasound, plays a crucial role in analyzing blood flow and velocity within arteries and veins (Hegner et al., 2023; Kizhisseri et al., 2023; Ponzini et al., 2010). Additionally, invasive methods like Fractional Flow Reserve (FFR) measurements are invaluable for assessing pressure drops across arterial stenoses, providing direct insights into the hemodynamic significance of lesions (Benz and Giannopoulos, 2020; Guo et al., 2024; Lee et al., 2022; Lo et al., 2020; Morris et al., 2015; Sanz Sánchez et al., 2023; Taylor et al., 2013; Tebaldi et al., 2015; Yan et al., 2024). In Figure 6, the use of coronary computed tomography angiography (CCTA) for the calculation of Fractional Flow Reserve is demonstrated. This imaging technique allows for a non-invasive assessment of coronary artery disease by

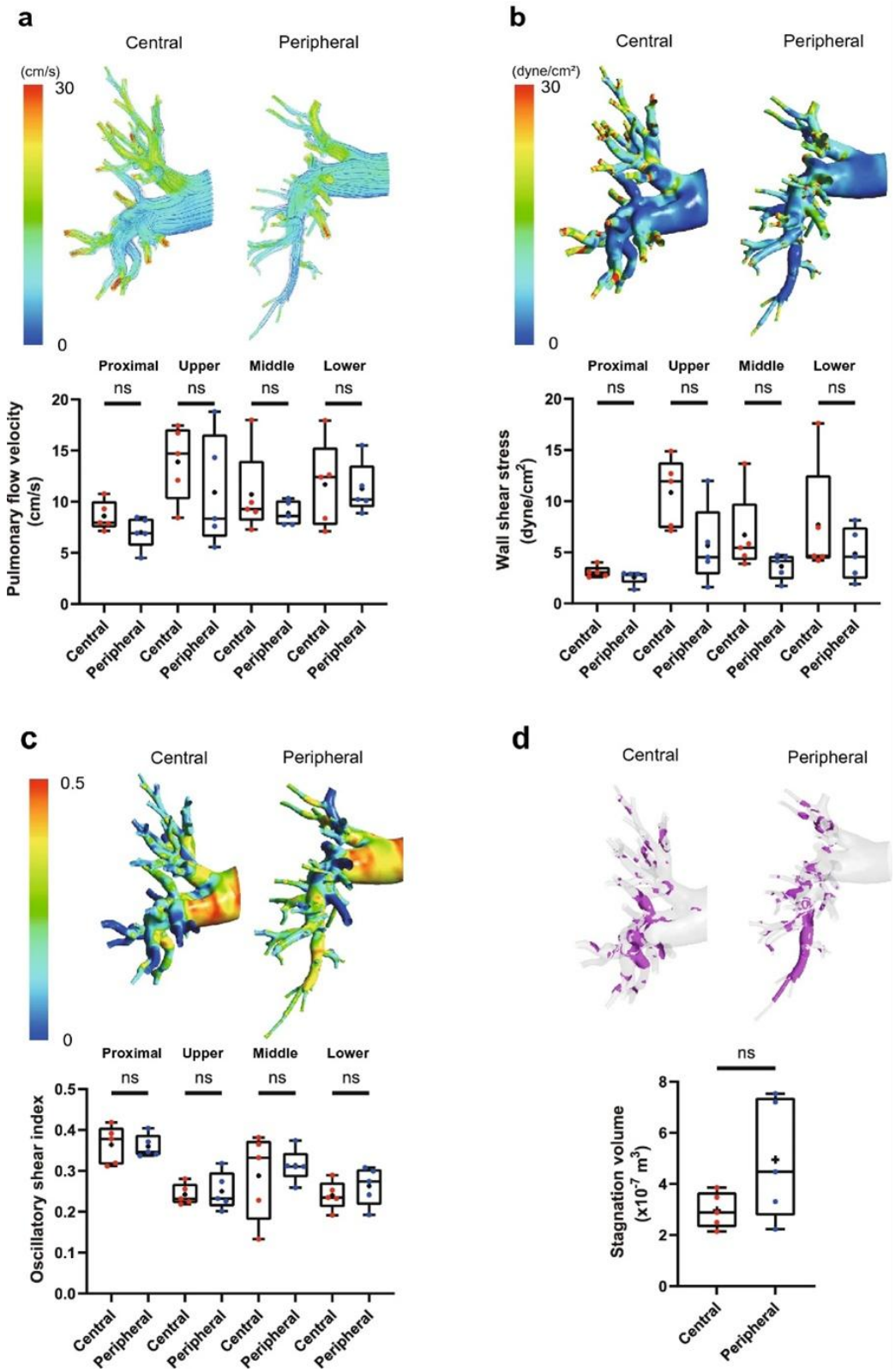

Figure 4. Comparison of pulmonary blood flow dynamics between central and peripheral type CTEPH. Pulmonary flow velocity (a), wall shear stress (b), oscillatory shear index (c), and blood stagnation volume (d) were simulated by CFD in the pulmonary arteries of patients with CTEPH in comparison with the central and peripheral types. Stagnation was defined as flow velocity of<0.01 m/s. Data are presented as median (interquartile range). Cross indicates mean. The numbers in each box plot indicate the sample size for each group. ns, not significant (Tsubata et al., 2023).

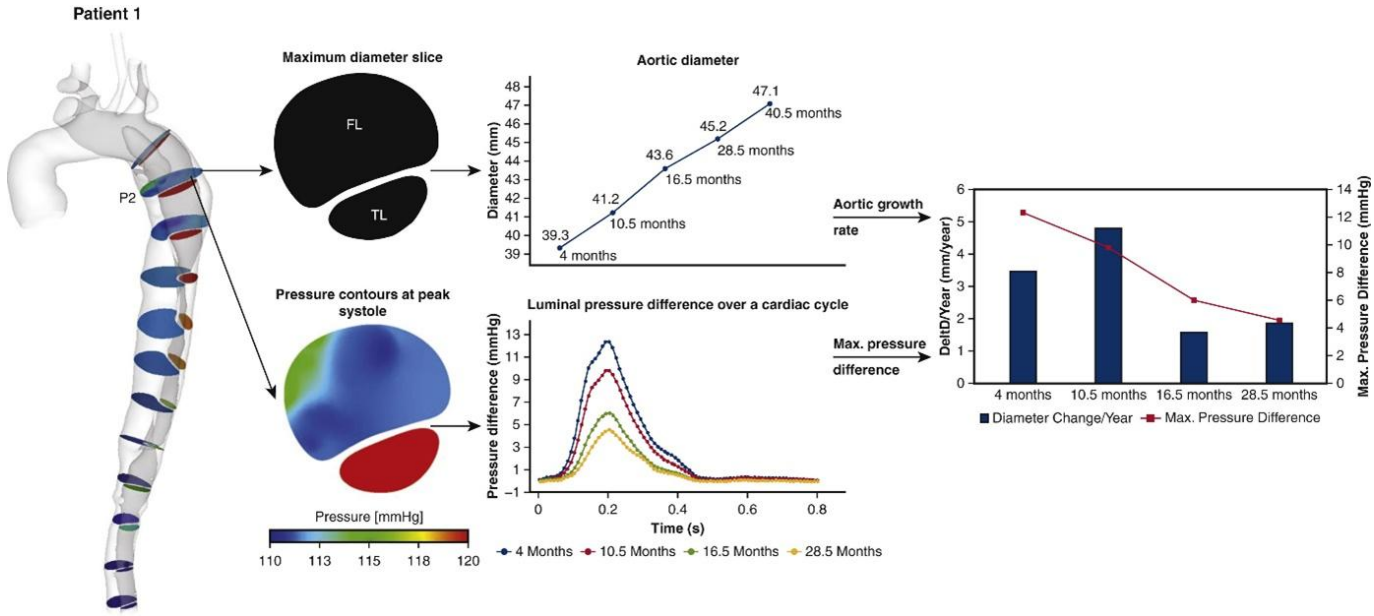

Figure 5. Illustration of aortic diameter changes of patient 1 (middle top) at a sample cross-sectional plane, namely the maximum diameter slice (P2). In addition, the spatial mean pressure variations over a cardiac cycle were calculated for the true lumen (TL) and false lumen (FL) separately, after which the pressure differences between 2 lumens were evaluated for each scan (middle bottom). Aortic growth rate (mm/year) at each follow-up scan, together with the maximum luminal pressure difference over a cardiac cycle were then evaluated and compared (right). The same procedure was repeated for all the other cross-sectional planes (Zhu et al., 2022). Copyright © 2022 Zhu Y., Xu X.Y., Rosendahl U., Pepper J., Mirsadraee S. Licensed under CC BY 4.0.

evaluating the severity of arterial stenosis and its impact on blood flow. As shown in Figure 6, the presence of a significant narrowing in the coronary artery results in a considerable drop in FFR, indicating a restriction in blood flow that could lead to ischemia. This highlights the clinical importance of FFR analysis in determining the functional significance of coronary stenosis and guiding treatment decisions.

An emerging technique that deserves special attention is 4D Flow Magnetic Resonance Imaging (4D Flow MRI) (Bissell et al., 2023; Dyverfeldt et al., 2015). This state-of-the-art imaging modality allows for a comprehensive analysis of blood flow throughout the cardiac cycle, capturing detailed hemodynamic parameters such as velocity fields, vorticity and wall shear stress in three-dimensional space over time. The data derived from 4D Flow MRI serves not only as a high-quality input for CFD simulations but also as a robust benchmark for validating these simulations. Figure 7 presents a comparison of the computational fluid dynamics (CFD) results and 4D Flow MRI data for a patient following the Fontan procedure. This three-step procedure is used, for example, in the case of hypoplasia of the left heart chamber, which is a lethal congenital defect. Ultimately, it results in the right ventricle functioning as the only ventricle – the main pump of blood. Blood is drawn through the pulmonary circulation from the right atrium to the left atrium, and then enters the right ventricle, from which it is pumped into the aorta. This comparison highlights the differences and similarities between the two imaging techniques in assessing the hemodynamics of the patient, providing valuable insights into blood flow patterns and potential complications after the procedure (Lee et al., 2023).

Its ability to capture dynamic changes during various phases of the heartbeat makes it a powerful tool for advancing personalized medicine and improving the accuracy of numerical models. Furthermore, the integration of these experimental and clinical data sources with numerical modeling can enhance our understanding of complex physiological phenomena, such as the development of arterial plaques, aneurysms, or turbulent blood flow in pathological conditions. Combining numerical modeling with experimental validation fosters the development of predictive tools for treatment planning, medical device design, and personalized therapies, ultimately bridging the gap between theoretical research and clinical application. Moreover, in the case of large intracerebral aneurysms, computational fluid dynamics has a particularly high potential for diagnosis and treatment planning, which is described in detail in the literature (Wiśniewski et al., 2024). In addition to Computational Fluid Dynamics (CFD) simulations, Fluid-Structure Interaction (FSI) simulations are increasingly employed. These simulations account for the movement of vessel walls, leading to deformation of the computational domain and enabling a more accurate analysis of hemodynamics. However, this increased accuracy comes at the cost of significantly higher computational demands. FSI simulations are particularly important in the study of blood flow within vessels that are subject to considerable deformation, both in the cardiovascular and respiratory systems (Wall and Rabczuk, 2008).

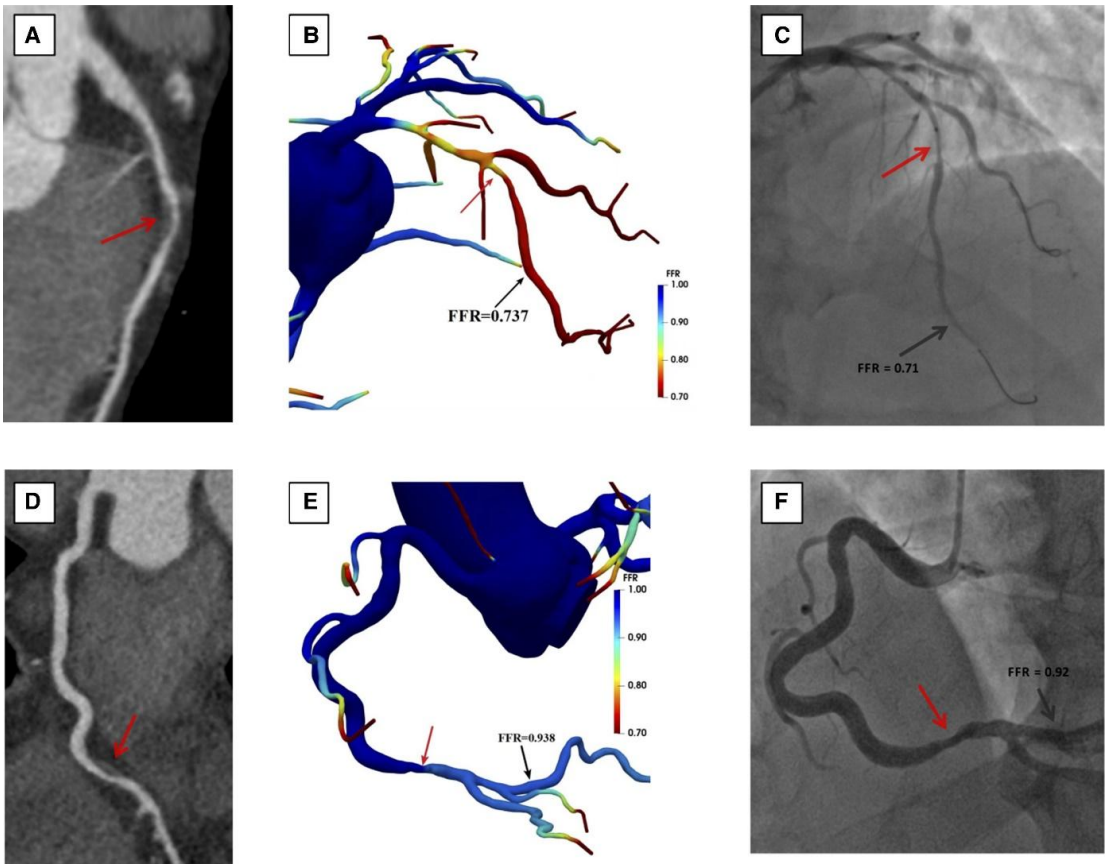

Figure 6. Case example. Two patients both with anatomically obstructive stenosis (arrow) on coronary computed tomography angiography (CCTA) (A and D). In the first patient (A–C), computation of fractional flow reserve from coronary computed tomography angiography (CT-FFR) demonstrates lesion-specific ischemia of the middle left anterior descending (LAD) stenosis, with a value of 0.74 (B). Invasive coronary angiography confirms the functionally obstructive stenosis with an invasive FFR of 0.71 (C). In the second patient (D–F), CT-FFR predicts no ischemia of the stenosis in the distal right coronary artery (RCA) with a CT-FFR value of 0.94 (E). Invasive FFR of 0.92 similarly demonstrates no ischemia of RCA (Guo et al., 2024).

It is also worth mentioning respiratory diseases such as Acute Respiratory Distress Syndrome (ARDS), where treatment often involves the use of Extracorporeal Membrane Oxygenation (ECMO). ECMO directly oxygenates the blood outside the body, bypassing the lungs and temporarily taking over their function (Gramigna et al., 2024; Parker et al., 2022, 2023, 2024). Although ARDS originates as a respiratory condition, the treatment approach involving ECMO shifts the focus in terms of CFD modeling closer to the circulatory system. ECMO systems present a unique challenge in CFD modeling due to the intricate interplay of fluid mechanics, hemocompatibility and device performance. These systems include components such as pumps, oxygenators and cannulas that must ensure efficient oxygenation while minimizing shear stress, turbulence, and hemolysis (Faghih and Sharp, 2019; Garon and Farinas, 2004; Jędrzejczak et al., 2023b). Accurate CFD simulations of ECMO systems require not only capturing the flow dynamics within the extracorporeal circuit but also accounting for physiological factors, such as patient-specific blood flow conditions, viscosity and interaction with native cardiovascular dynamics. From the modeling perspective, the inclusion of ECMO in ARDS treatment introduces complexities such as the need to simulate blood flow under varying flow rates and oxygenation levels. Figure 8 illustrates the application of CFD in analyzing the changes in blood flow dynamics during Extracorporeal Membrane Oxygenation (Parker et al., 2024).

The interaction between the ECMO circuit and the patient's heart and lungs is critical, as any mismatch can lead to complications such as recirculation, thrombosis or hemodynamic instability. These aspects necessitate advanced multi-scale modeling that integrates the extracorporeal circuit with the native circulatory system to provide a comprehensive picture. Moreover, experimental validation is essential in this context. Benchtop testing using physical models of ECMO circuits combined with PIV measurements can offer insights into flow patterns, pressure drops, and oxygenation efficiency (Fiusco et al., 2023; Zhang et al., 2020).

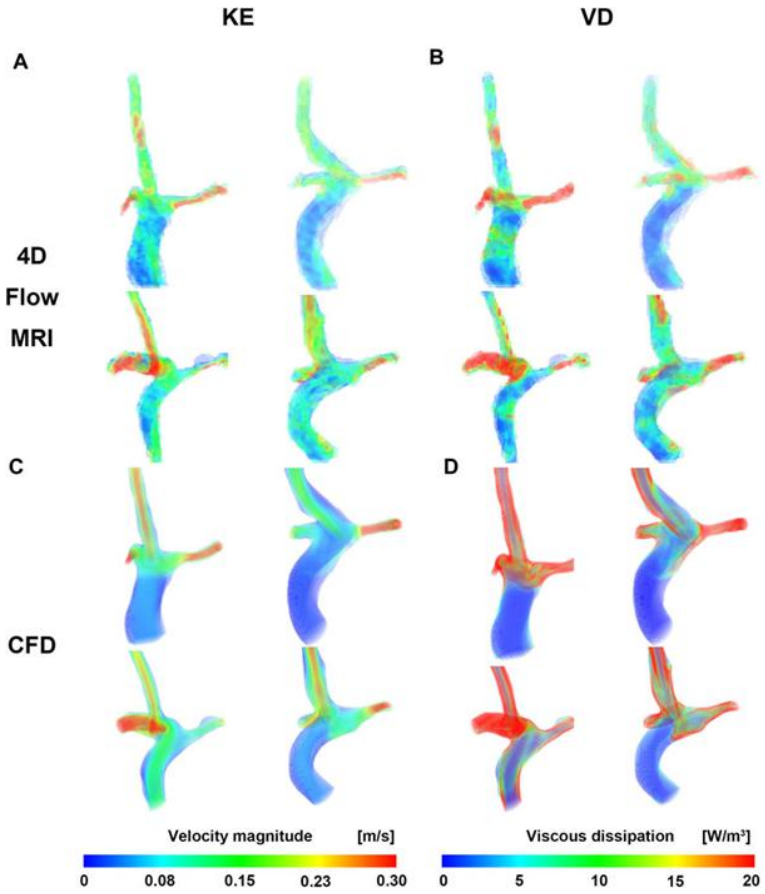

Figure 7. Velocity and viscous dissipation contour. (A) Velocity of CFD. (B) Viscous dissipation of CFD. (C) Velocity of 4D Flow MRI. (D) Viscous dissipation of 4D Flow MRI (Lee et al., 2023). Copyright © 2023 Lee G.-H., Koo H.J., Park K.J., Yang D.H., Ha H. Licensed under CC BY 4.0.

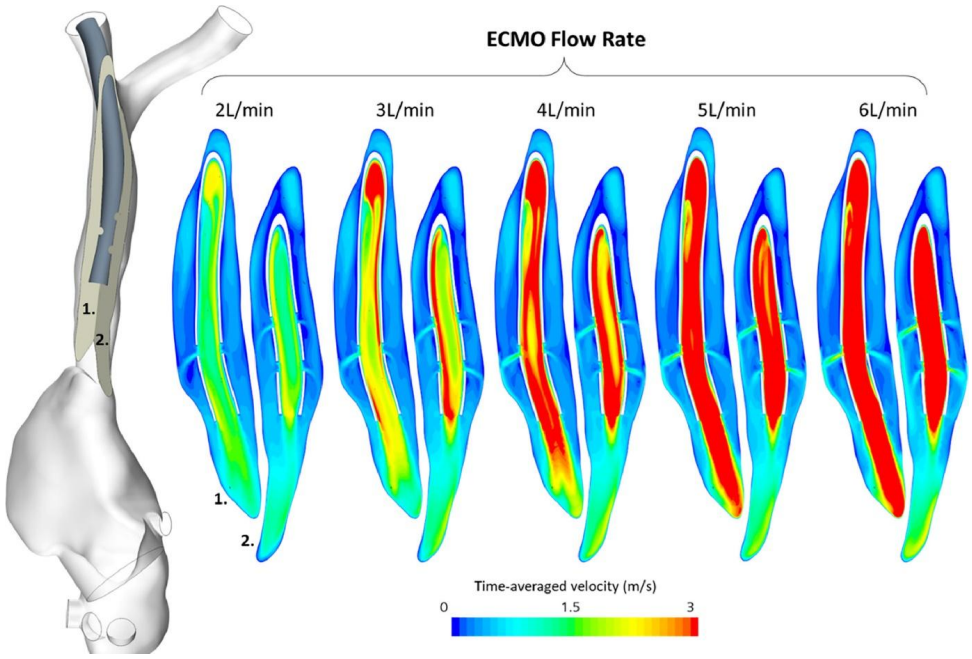

Figure 8. Time-averaged velocity shown on two cross-sectional planes through the return cannula, at 5 L/min total cardiac output and for ECMO flow rates from 2 to 6 L/min. (Parker et al., 2024). Copyright © 2024 Parker L.P., Svensson Marcial A., Brismar T.B., Broman L.M., Prahl Wittberg L. Licensed under CC BY 4.0.

3.3. Artificial intelligence in modeling respiratory and circulatory systems

Artificial intelligence is increasingly used to analyze medical imaging data (Ferdian et al., 2020, 2023) and is being integrated with CFD to speed up flow predictions. The growing interest in AI combined with CFD is also visible in the increase in the number of publications on this topic (Praharaj et al., 2024). Artificial neural networks can be trained using detailed CFD simulations to quickly predict airflow or blood flow, which is useful in real-time clinical settings or for optimizing medical devices (Lv et al., 2022). AI is also playing a growing role in supporting doctors in disease detection and diagnosis by analyzing complex data, such as medical images or multi-scale datasets, to identify patterns and create better clinical guidelines (Akyüz et al., 2024; Alowais et al., 2023; Arora et al., 2023). It helps tailor treatments to individual patients by analyzing their specific conditions (Samant et al., 2023). AI also aids in predicting disease progression and treatment outcomes, enabling personalized care by forecasting how a patient's condition will evolve (Starling et al., 2024). Additionally, AI is being used to create virtual research environments where medical devices and treatments can be tested safely before clinical trials (Tsuchiwata and Tsuji, 2023). In all these ways, AI is transforming the medical field by providing faster, more accurate predictions, personalized treatments and new insights that were previously impossible to achieve.

4. CONCLUSIONS

Computational fluid dynamics and artificial intelligence are transforming modern medicine by improving diagnostics, treatment planning and patient care. Advances in computing power have made these technologies more accessible, reducing costs while enhancing accuracy and efficiency. CFD is crucial in studying cardiovascular and respiratory systems, enabling simulations of blood flow and airflow to predict disease progression and optimize treatments. It also aids in designing medical devices like stents, ventilators, and inhalers. AI, particularly machine learning and deep learning, enhances medical imaging, detecting heart and lung diseases with high accuracy. AI-driven models improve ventilator performance, diagnostics, and predictive analytics, leading to earlier interventions and better patient outcomes. As these technologies evolve, their integration into healthcare will enable real-time simulations, AI-assisted surgeries, and personalized medicine, ultimately improving efficiency and reducing healthcare costs.

REFERENCES

Ahadi F., Biglari M., Azadi M., Bodaghi M., 2024. Computational fluid dynamics of coronary arteries with implanted stents: Effects of Newtonian and non-Newtonian blood flows. *Eng. Rep.*, 6, e12779. DOI: 10.1002/eng2.12779.

Ait Ali L., Martini N., Listo E., Valenti E., Sotelo J., Salvadori S., Passino C., Monteleone A., Stagnaro N., Trocchio G., Marrone C., Raimondi F., Catapano G., Festa P., 2024. Impact of 4D-flow CMR parameters on functional evaluation of fontan circulation. *Pediatr. Cardiol.*, 45, 998–1006. DOI: 10.1007/s00246-024-03446-4.

Akor E.A., Han B., Cai M., Lin C.-L., Kaczka D.W., 2024. Forward computational modeling of respiratory airflow. *Appl. Sci.*, 14, 11591. DOI: 10.3390/app142411591.

Akyüz K., Cano Abadía M., Goisauf M., Mayrhofer M.Th., 2024. Unlocking the potential of big data and AI in medicine: insights from biobanking. *Front. Med.*, 11, 1336588. DOI: 10.3389/fmed.2024.1336588.

Aliboni L., Tullio M., Pennati F., Lomauro A., Carrinola R., Carrafiello G., Nosotti M., Palleschi A., Aliverti A., 2022. Functional analysis of the airways after pulmonary lobectomy through computational fluid dynamics. *Sci. Rep.*, 12, 3321. DOI: 10.1038/s41598-022-06852-x.

Alowais S.A., Alghamdi S.S., Alsuhebany N., Alqahtani T., Alshaya A.I., Almohareb S.N., Aldairem A., Alrashed M., Bin Saleh K., Badreldin H.A., Al Yami M.S., Al Harbi S., Albekairy A.M., 2023. Revolutionizing healthcare: the role of artificial intelligence in clinical practice. *BMC Med. Educ.*, 23, 689. DOI: 10.1186/s12909-023-04698-z.

Antonowicz A., Wojtas K., Makowski Ł., Orciuch W., Kozłowski M., 2023. Particle image velocimetry of 3D-printed anatomical blood vascular models affected by atherosclerosis. *Materials*, 16, 1055. DOI: 10.3390/ma16031055.

Arminio M., Carbonaro D., Morbiducci U., Gallo D., Chiastra C., 2024. Fluid-structure interaction simulation of mechanical aortic valves: a narrative review exploring its role in total product life cycle. *Front. Med. Technol.*, 6, 1399729. DOI: 10.3389/fmedt.2024.1399729.

Arora A., Alderman J.E., Palmer J., Ganapathi S., Laws E., McCradden M.D., Oakden-Rayner L., Pfohl S.R., Ghassemi M., McKay F., Treanor D., Rostamzadeh N., Mateen B., Gath J., Adebajo A.O., Kuku S., Matin R., Heller K., Sapey E., Sebire N.J., Cole-Lewis H., Calvert M., Denniston A., Liu X., 2023. The value of standards for health datasets in artificial intelligence-based applications. *Nat. Med.*, 29, 2929–2938. DOI: 10.1038/s41591-023-02608-w

Bao Y., Qu S., Li K., 2022. Investigation and analysis of the influence of vegetative tracheobronchial foreign body on airflow field. *Appl. Bionics Biomech.*, 2022, 8930283. DOI: 10.1155/2022/8930283.

Benz D.C., Giannopoulos A.A., 2020. Fractional flow reserve as the standard of reference: *All that glistens is not gold. J. Nucl. Cardiol.*, 27, 1314–1316. DOI: 10.1007/s12350-019-01771-3.

Białecki R., Adamczyk W., Ostrowski Z., 2024. Selected aspects of blood flow simulations in arteries. *Arch. Thermodyn.*, 45, 145–153. DOI: 10.24425/ather.2024.150447

Bissell M.M., Raimondi F., Ait Ali L., Allen B.D., Barker A.J., Bolger A., Burris N., Carhäll C.-J., Collins J.D., Ebbers T., Francois C.J., Frydrychowicz A., Garg P., Geiger J., Ha H., Hennemuth A., Hope M.D., Hsiao A., Johnson K., Kozerke S., Ma L.E., Markl M., Martins D., Messina M., Oechtering T.H.,

van Ooij P., Rigsby C., Rodriguez-Palomares J., Roest A.A.W., Roldán-Alzate A., Schnell S., Sotelo J., Stuber M., Syed A.B., Töger J., van der Geest R., Westenberg J., Zhong L., Zhong Y., Wieben O., Dyverfeldt P., 2023. 4D Flow cardiovascular magnetic resonance consensus statement: 2023 update. *J. Cardiovasc. Magn. Reson.*, 25, 40. DOI: 10.1186/s12968-023-00942-z.

Boite Y., Suaiden Klein T., de Andrade Medronho R., Wajnberg E., 2023. Numerical simulation of flow-diverting stent: comparison between branches in bifurcation brain aneurysm. *Biomech. Model. Mechanobiol.*, 22, 1801–1814. DOI: 10.1007/s10237-023-01733-2.

Burgos M.A., Rosique L., Piqueras F., García-Navalón C., Sevilla-García M.A., Hellín D., Esteban F., 2024. Reducing variability in nasal surgery outcomes through computational fluid dynamics and advanced 3D virtual surgery techniques. *Heliyon*, 10, e26855. DOI: 10.1016/j.heliyon.2024.e26855.

Chaichana T., Sun Z., Jewkes J., 2012. Computational fluid dynamics analysis of the effect of plaques in the left coronary artery. *Comput. Math. Methods Med.*, 2012, 504367. DOI: 10.1155/2012/504367.

Chen W.X., Poon E.K.W., Hutchins N., Thondapu V., Barlis P., Ooi A., 2017. Computational fluid dynamics study of common stent models inside idealised curved coronary arteries. *Comput. Methods Biomech. Biomed. Eng.*, 20, 671–681. DOI: 10.1080/10255842.2017.1289374.

Chen X., Cao H., Li Y., Chen F., Peng Y., Zheng T., Chen M., 2024. Hemodynamic influence of mild stenosis morphology in different coronary arteries: a computational fluid dynamic modelling study. *Front. Bioeng. Biotechnol.*, 12, 1439846. DOI: 10.3389/fbioe.2024.1439846.

Chen Z., Qin H., Liu J., Wu B., Cheng Z., Jiang Y., Liu L., Jing L., Leng X., Jing J., Wang Y., Wang Y., 2020. Characteristics of wall shear stress and pressure of intracranial atherosclerosis analyzed by a computational fluid dynamics model: A pilot study. *Front. Neurol.*, 10, 1372. DOI: 10.3389/fneur.2019.01372.

Chiastra C., Zuin M., Rigatelli G., D'Ascenzo F., De Ferrari G.M., Collet C., Chatzizisis Y.S., Gallo D., Morbiducci U., 2023. Computational fluid dynamics as supporting technology for coronary artery disease diagnosis and treatment: an international survey. *Front. Cardiovasc. Med.*, 10, 1216796. DOI: 10.3389/fcvm.2023.1216796.

Chiu T.L., Tang A.Y.S., Cheng S.W.K., Chow K.W., 2018. Analysis of flow patterns on branched endografts for aortic arch aneurysms. *Inf. Med. Unlocked*, 13, 62–70. DOI: 10.1016/j.imu.2018.10.008.

Cieślicki K., Ciszek B., Lasowska A., Smolarski A., 2002. Modelling of flow in a network structure of the main cerebral arteries. *Arch. Biol. Sci.*, 50(4), 25–35.

Ciołkowski M., Sharifi M., Tarka S., Ciszek B., 2011. Median aperture of the fourth ventricle revisited. *Folia Morphol. (Warsz).*, 70, 84–90.

Ciszek B., Cieślicki K., Krajewski P., Piechnik S.K., 2013. Critical pressure for arterial wall rupture in major human cerebral arteries. *Stroke*, 44, 3226–3228. DOI: 10.1161/STROKEAHA.113.002370.

Collier G.J., Kim M., Chung Y., Wild J.M., 2018. 3D phase contrast MRI in models of human airways: Validation of computational fluid dynamics simulations of steady inspiratory flow. *J. Magn. Reson. Imaging*, 48, 1400–1409. DOI: doi.org/10.1002/jmri.26039.

Conijn M., Krings G.J., 2022. Understanding stenotic pulmonary arteries: Can computational fluid dynamics help us out? *Prog. Pediatr. Cardiol.*, 64, 101452. DOI: 10.1016/j.ppedcard.2021.101452.

De Backer J.W., Vos W.G., Devolder A., Verhulst S.L., Germonpré P., Wuyts F.L., Parizel P.M., De Backer W., 2008. Computational fluid dynamics can detect changes in airway resistance in asthmatics after acute bronchodilation. *J. Biomech.*, 41, 106–113. DOI: 10.1016/j.jbiomech.2007.07.009.

De Nisco G., Chiastra C., Hartman E.M.J., Hoogendoorn A., Daemen J., Calò K., Gallo D., Morbiducci U., Wentzel J.J., 2021. Comparison of swine and human computational hemodynamics models for the study of coronary atherosclerosis. *Front. Bioeng. Biotechnol.*, 9, 731924. DOI: 10.3389/fbioe.2021.731924.

Dedè L., Menghini F., Quarteroni A., 2021. Computational fluid dynamics of blood flow in an idealized left human heart. *Int. J. Numer. Meth. Biomed. Engng.*, 37, e3287. DOI: 10.1002/cnm.3287.

Dyverfeldt P., Bissell M., Barker A.J., Bolger A.F., Carlhäll C.-J., Ebbers T., Francios C.J., Frydrychowicz A., Geiger J., Giese D., Hope M.D., Kilner P.J., Kozerke S., Myerson S., Neubauer S., Wieben O., Markl M., 2015. 4D flow cardiovascular magnetic resonance consensus statement. *J. Cardiovasc. Magn. Reson.*, 17, 72. DOI: 10.1186/S12968-015-0174-5.

Ekmejian A.A., Carpenter H.J., Ciofani J.L., Gray B.H.M., Allahwala U.K., Ward M., Escaned J., Psaltis P.J., Bhindi R., 2024. Advances in the Computational Assessment of Disturbed Coronary Flow and Wall Shear Stress: A Contemporary Review. *J. Am. Heart Assoc.*, 13, e037129. DOI: 10.1161/JAHA.124.037129.

Faghih M.M., Sharp M.K., 2019. Modeling and prediction of flow-induced hemolysis: a review. *Biomech. Model. Mechanobiol.*, 18, 845–881. DOI: 10.1007/s10237-019-01137-1.

Ferdian E., Marlevi D., Schollenberger J., Aristova M., Edelman E.R., Schnell S., Figueroa C.A., Nordsletten D.A., Young A.A., 2023. Cerebrovascular super-resolution 4D Flow MRI – Sequential combination of resolution enhancement by deep learning and physics-informed image processing to non-invasively quantify intracranial velocity, flow, and relative pressure. *Med. Image Anal.*, 88, 102831. DOI: 10.1016/j.media.2023.102831.

Ferdian E., Suinesiaputra A., Dubowitz D.J., Zhao D., Wang A., Cowan B., Young A.A., 2020. 4DFlowNet: Super-Resolution 4D Flow MRI Using Deep Learning and Computational Fluid Dynamics. *Front. Phys.*, 8, 138. DOI: 10.3389/fphy.2020.00138

Fiusco F., Lemétayer J., Broman L.M., Prahl Wittberg L., 2023. Effect of flow rate ratio and positioning on a lighthouse tip ECMO return cannula. *Biomech. Model. Mechanobiol.*, 22, 1891–1899. DOI: 10.1007/s10237-023-01741-2.

Gamrot-Wrzoł M., Marków M., Janecki D., Misiołek M., 2020. The suitability of CFD in diagnosis and treatment of laryngeal diseases. *Pol. Otorhino. Rev.*, 9, 23–26. DOI: 10.5604/01.3001.0014.0995.

Gao W., Yin C., Zhou C., Cheng D., Chen J., Liu C., Zeng Y., 2025. Hemodynamic investigations on the portal hypertension and treatment of transjugular intrahepatic portosystemic shunt (TIPS) based on CFD simulation. *J. Biomech.*, 181, 112516. DOI: 10.1016/J.JBIOMECH.2025.112516.

Garon A., Farinas M.-I., 2004. Fast Three-dimensional Numerical Hemolysis Approximation. *Artif. Organs*, 28, 1016–1025. DOI: 10.1111/j.1525-1594.2004.00026.x.

Ghafarian P., Jamaati H., Hashemian S.M., 2016. A review on human respiratory modeling. *TANAFFOS (Respiration)*, 15, 61–69.

Gramigna V., Palumbo A., Fragomeni G., 2024. The influence of different ecmo cannulation site and blood perfusion conditions on the aortic hemodynamics: A Computational Fluid Dynamic model. *Fluids*, 9, 269. DOI: 10.3390/fluids9110269.

Guo W., He W., Lu Y., Yin J., Shen L., Yang S., Jin H., Wang X., Jun J., Hu X., Liang J., Wei W., Wu J., Zhang H., Zhou H., Wu Y., Yang R., Huang J., Tong G., Gao B., Chen R., Liu J., Yan Z., Cheng Z., Wang J., Li C., Yao Z., Zeng M., Ge J., 2024. CT-FFR by expanding coronary tree with Newton–Krylov–Schwarz method to solve the governing equations of CFD. *Eur. Heart J. Imaging Methods Pract.*, 2, qyae106. DOI: 10.1093/ehjimp/qyae106.

Han K., Lee S.G., Kim K., Jeong B., Paek M., Lee W., Hwang W., 2023. Investigation of the effects of nasal surgery on nasal cavity flow using magnetic resonance velocimetry and computational fluid dynamics. *Phys. Fluids*, 35, 111908. DOI: 10.1063/5.0169775.

Hegner A., Wittek A., Derwich W., Huß A., Gámez A.J., Blase C., 2023. Using averaged models from 4D ultrasound strain imaging allows to significantly differentiate local wall strains in calcified regions of abdominal aortic aneurysms. *Biomech. Model. Mechanobiol.*, 22, 1709–1727. DOI: 10.1007/ s10237-023-01738-x.

Ho W.H., Tshimanga I.J., Ngoepe M.N., Jermy M.C., Geoghegan P.H., 2020. Evaluation of a desktop 3D printed rigid refractive-indexed-matched flow phantom for PIV measurements on cerebral aneurysms. *Cardiovasc. Eng. Technol.*, 11, 14–23. DOI: 10.1007/s13239-019-00444-z.

Hoganson D.M., Govindarajan V., Schulz N.E., Eickhoff E.R., Breitbart R.E., Marx G.R., del Nido P.J., Hammer P.E., 2024. Multiphysiologic state computational fluid dynamics modeling for planning Fontan with interrupted inferior vena cava. *JACC Adv.*, 3, 101057. DOI: 10.1016/j.jacadv.2024.101057.

Hu B., Yin G., Fu S., Zhang B., Shang Y., Zhang Y., Ye J., 2023. The influence of mouth opening on pharyngeal pressure loss and its underlying mechanism: A computational fluid dynamic analysis. *Front. Bioeng. Biotechnol.*, 10, 1081465. DOI: 10.3389/fbioe.2022.1081465.

Hudson T.J., Ait Oubahou R., Mongeau L., Kost K., 2023. Airway resistance and respiratory distress in laryngeal cancer: A computational fluid dynamics study. *Laryngoscope*, 133, 2734–2741. DOI: 10.1002/lary.30649.

Jankowska-Steifer E., Ratajska A., Czarnowska E., Badurek I., Matryba P., Niderla-Bielińska J., Ciszek B., Brakenhielm E., 2021. Assessing functional status of cardiac lymphatics: From macroscopic imaging to molecular profiling. *Trends Cardiovasc. Med.*, 31, 333–338. DOI: 10.1016/j.tcm.2020.06.006.

Jansen I.G.H., Schneiders J.J., Potters W.V., Van Ooij P., van den Berg R., van Bavel E., Marquering H.A., Majoie C.B.L.M., 2014. Generalized versus patient-specific inflow boundary conditions in computational fluid dynamics simulations of cerebral aneurysmal hemodynamics. *Am. J. Neuroradiol.*, 35, 1543–1548. DOI: 10.3174/ajnr.A3901.

Jayendiran R., Nour B., Ruimi A., 2018. Fluid-structure interaction (FSI) analysis of stent-graft for aortic endovascular aneurysm repair (EVAR): Material and structural considerations. *J. Mech. Behav. Biomed. Mater.*, 87, 95–110. DOI: 10.1016/J.JMBBM.2018.07.020.

Jędrzejczak K., Antonowicz A., Makowski Ł., Orciuch W., Wojtas K., Kozłowski M., 2023a. Computational fluid dynamics validated by micro particle image velocimetry to estimate the risk of hemolysis in arteries with atherosclerotic lesions. *Chem. Eng. Res. Des.*, 196, 342–353. DOI: 10.1016/j.cherd.2023.06.041.

Jędrzejczak K., Makowski Ł., Orciuch W., 2023b. Model of blood rheology including hemolysis based on population balance. *Commun. Nonlinear Sci. Numer. Simul.*, 116, 106802. DOI: 10.1016/J.CNSNS.2022.106802

Jędrzejczak K., Makowski Ł., Orciuch W., Wojtas K., Kozłowski M., 2023c. Hemolysis of red blood cells in blood vessels modeled via computational fluid dynamics. *Int. J. Numer. Method. Biomed. Eng.*, 39, e3699. DOI: 10.1002/cnm.3699.

Jędrzejczak K., Orciuch W., Wojtas K., Kozłowski M., Piasecki P., Narloch J., Wierzbicki M., Makowski Ł., 2024a. Prediction of hemodynamic-related hemolysis in carotid stenosis and aiding in treatment planning and risk stratification using computational fluid dynamics. *Biomedicines*, 12, 37. DOI: 10.3390/biomedicines12010037.

Jędrzejczak K., Orciuch W., Wojtas K., Piasecki P., Narloch J., Wierzbicki M., Kozłowski M., Bissell M.M., Makowski Ł., 2024b. Impact of hypertension and physical exercise on hemolysis risk in the left coronary artery: A computational fluid dynamics analysis. *J. Clin. Med.*, 13, 6163. DOI: 10.3390/jcm13206163.

Jeong S.J., Kim W.S., Sung S.J., 2007. Numerical investigation on the flow characteristics and aerodynamic force of the upper airway of patient with obstructive sleep apnea using computational fluid dynamics. *Med. Eng. Phys.*, 29, 637–651. DOI: 10.1016/j.medengphy.2006.08.017.

Karmonik C., Partovi S., Davies M.G., Bismuth J., Shah D.J., Bilecen D., Staub D., Noon G.P., Loebe M., Bongartz G., Lumsden A.B., 2013. Integration of the computational fluid dynamics technique with MRI in aortic dissections. *Magn. Reson. Med.*, 69, 1438–1442. DOI: 10.1002/mrm.24376.

Kasiteropoulou D., Topalidou A., Downe S., 2020. A computational fluid dynamics modelling of maternal-fetal heat exchange and blood flow in the umbilical cord. *PLoS One*, 15, e0231997. DOI: 10.1371/journal.pone.0231997.

Kim H.J., Vignon-Clementel I.E., Coogan J.S., Figueroa C.A., Jansen K.E., Taylor C.A., 2010. Patient-specific modeling of blood flow and pressure in human coronary arteries. *Ann. Biomed. Eng.*, 38, 3195–3209. DOI: 10.1007/s10439-010-0083-6.

Kizhisseri M., Gharaie S., Schluter J., 2023. An analytical method informed by clinical imaging data for estimating outlet boundary conditions in computational fluid dynamics analysis of carotid artery blood flow. *Sci. Rep.*, 13, 14973. DOI: 10.1038/s41598-023-42004-5

Kozłowski M., Wojtas K., Orciuch W., Jędrzejek M., Smolka G., Wojakowski W., Makowski Ł., 2021. Potential applications of computational fluid dynamics for predicting hemolysis in mitral paravalvular leaks. *J. Clin. Med.*, 10, 5752. DOI: 10.3390/jcm10245752.

Kozłowski M., Wojtas K., Orciuch W., Smolka G., Wojakowski W., Makowski Ł., 2022. Parameters of flow through paravalvular leak channels from computational fluid dynamics simulations–data from real-life cases and comparison with a simplified model. *J. Clin. Med.*, 11, 5355. DOI: 10.3390/jcm11185355.

Kuprat A.P., Jalali M., Jan T., Corley R.A., Asgharian B., Price O., Singh R.K., Colby S., Darquenne C., 2021. Efficient bi-directional coupling of 3D computational fluid-particle dynamics and 1D Multiple Path Particle Dosimetry lung models for multiscale modeling of aerosol dosimetry. *J. Aerosol Sci.*, 151, 105647. DOI: 10.1016/j.jaerosci.2020.105647

Lee G.-H., Koo H.J., Park K.J., Yang D.H., Ha H., 2023. Characterization of baseline hemodynamics after the Fontan procedure: a retrospective cohort study on the comparison of 4D Flow MRI and computational fluid dynamics. *Front. Physiol.*, 14, 1199771. DOI: 10.3389/fphys.2023.1199771.

Lee H.J., Kim Y.W., Kim J.H., Lee Y.-J., Moon J., Jeong P., Jeong J., Kim J.-S., Lee J.S., 2022. Optimization of FFR prediction algorithm for gray zone by hemodynamic features with synthetic model and biometric data. *Comput. Methods Programs Biomed.*, 220, 106827. DOI: 10.1016/J.CMPB.2022.106827.

Li Y., Verrelli D.I., Yang W., Qian Y., Chong W., 2020. A pilot validation of CFD model results against PIV observations of haemodynamics in intracranial aneurysms treated with flow-diverting stents. *J. Biomech.*, 100, 109590. DOI: 10.1016/j.jbiomech.2019.109590.

Lo E.W.C., Menezes L.J., Torii R., 2020. On outflow boundary conditions for CT-based computation of FFR: Examination using PET images. *Med. Eng. Phys.*, 76, 79–87. DOI: 10.1016/j.medengphy.2019.10.007.

Luisi C.A., Witter T.L., Nikoubashman O., Wiesmann M., Steinseifer U., Neidlin M., 2024. Evaluating the accuracy of cerebrovascular computational fluid dynamics modeling through time-resolved experimental validation. *Sci. Rep.*, 14, 8194. DOI: 10.1038/s41598-024-58925-8.

Lv L., Li H., Wu Z., Zeng W., Hua P., Yang S., 2022. An artificial intelligence-based platform for automatically estimating time-averaged wall shear stress in the ascending aorta. *Eur. Heart J. Digital Health*, 3, 525–534. DOI: 10.1093/ehjdh/ztac058.

Malec E., Schmidt C., Lehner A., Januszewska K., 2017. Results of the Fontan operation with no early mortality in 248 consecutive patients. *Kardiol. Pol.*, 75, 255–260. DOI: 10.5603/KP.a2016.0170.

Milewski M., Koh E.L., Gąsior P., Lian S.S., Yinling Z., Pawłowski T., Foin N., Khedi E., Wojakowski W., Ang H.Y., 2024. Provisional stenting technique in the left main bifurcation setting: Computational fluid dynamics and optical coherence tomography pilot study in humans. *Pol. Heart J.*, 82, 651–653. DOI: 10.33963/v.phj.100572.

Morbiducci U., Mazzi V., Domanin M., De Nisco G., Vergara C., Steinman D.A., Gallo D., 2020. Wall shear stress topological skeleton independently predicts long-term restenosis after carotid bifurcation endarterectomy. *Ann. Biomed. Eng.*, 48, 2936–2949. DOI: 10.1007/s10439-020-02607-9.

Morris P.D., van de Vosse F.N., Lawford P.V, Hose D.R., Gunn J.P., 2015. "Virtual" (computed) fractional flow reserve: current challenges and limitations. *JACC Cardiovasc. Interv.*, 8, 1009–1017. DOI: 10.1016/j.jcin.2015.04.006.

Mylavarapu G., Mihaescu M., Fuchs L., Papatziamos G., Gutmark E., 2013. Planning human upper airway surgery using computational fluid dynamics. *J. Biomech.*, 46, 1979–1986. DOI: 10.1016/j.jbiomech.2013.06.016.

Mylavarapu G., Murugappan S., Mihaescu M., Kalra M., Khosla S., Gutmark E., 2009. Validation of computational fluid dynamics methodology used for human upper airway flow simulations. *J. Biomech.*, 42, 1553–1559. DOI: 10.1016/j.jbiomech.2009.03.035.

Na Y., Kim Y.-J., Kim H.Y., Jung Y.G., 2022. Improvements in airflow characteristics and effect on the NOSE score after septoturbinoplasty: A computational fluid dynamics analysis. *PLoS One*, 17, e0277712. DOI: 10.1371/journal.pone.0277712.

Ninke T., Eifer A., Dieterich H.-J., Groene P., 2024. Besonderheiten des fetalen und kindlichen Atmungssystems. *Anaesthesiologie*, 73, 65–74. DOI: 10.1007/s00101-023-01364-3.

Nishijima H., Kondo K., Yamamoto T., Nomura T., Kikuta S., Shimizu Y., Mizushima Y., Yamasoba T., 2018. Influence of the location of nasal polyps on olfactory airflow and olfaction. *Int. Forum Allergy Rhinol.*, 8, 695–706. DOI: 10.1002/alr.22089.

Ormiskangas J., Valtonen O., Harju T., Rautiainen M., Kivekäs I., 2022. Computational fluid dynamics assessed changes of nasal airflow after inferior turbinate surgery. *Respir. Physiol. Neurobiol.*, 302, 103917. DOI: 10.1016/J.RESP.2022.103917

Park H., Yeom E., Lee S.J., 2016. X-ray PIV measurement of blood flow in deep vessels of a rat: An *in vivo* feasibility study. *Sci. Rep.*, 6, 19194. DOI: 10.1038/srep19194.

Parker L.P., Marcial A.S., Brismar T.B., Broman L.M., Prahl Wittberg L., 2022. Cannulation configuration and recirculation in venovenous extracorporeal membrane oxygenation. *Sci. Rep.*, 12, 16379. DOI: 10.1038/s41598-022-20690-x.

Parker L.P., Svensson Marcial A., Brismar T.B., Broman L.M., Prahl Wittberg L., 2024. *In silico* parametric analysis of femoro-jugular venovenous ECMO and return cannula dynamics. *Med. Eng. Phys.*, 125, 104126. DOI: 10.1016/j.medengphy.2024.104126.

Parker L.P., Svensson Marcial A., Brismar T.B., Broman L.M., Prahl Wittberg L., 2023. Hemodynamic and recirculation performance of dual lumen cannulas for venovenous extracorporeal membrane oxygenation. *Sci. Rep.*, 13, 7472. DOI: 10.1038/s41598-023-34655-1.

Patwa A., Shah A., 2015. Anatomy and physiology of respiratory system relevant to anaesthesia. *Indian J. Anaesth.*, 59, 533–541. DOI: 10.4103/0019-5049.165849.

Paz C., Suárez E., Vence J., 2017. CFD transient simulation of the cough clearance process using an Eulerian wall film model. *Comput. Methods Biomech. Biomed. Engin.*, 20, 142–152. DOI: 10.1080/10255842.2016.1206532.

Pennati G., Corsini C., Hsia T.-Y., Migliavacca F., 2013. Computational fluid dynamics models and congenital heart diseases. *Front. Pediatr.*, 1, 4. DOI: 10.3389/fped.2013.00004.

Phuong N.L., Ito K., 2015. Investigation of flow pattern in upper human airway including oral and nasal inhalation by PIV and CFD. *Build. Environ.*, 94, 504–515. DOI: 10.1016/j.buildenv.2015.10.002.

Piechna A., Lombarski L., Ciszek B., Cieslicki K., 2017. Experimental determination of rupture pressure and stress of adventitia of human middle cerebral arteries. *Int. J. Stroke*, 12, 636–640. DOI: 10.1177/1747493016685715.

Pirnar J., Dolenc-Grošelj L., Fajdiga I., Žun I., 2015. Computational fluid-structure interaction simulation of airflow in the human upper airway. *J. Biomech.*, 48, 3685–3691. DOI: 10.1016/j.jbiomech.2015.08.017.

Polaczek M., Szaro P., Baranska I., Burakowska B., Ciszek B., 2019. Morphology and morphometry of pulmonary veins and the left atrium in multi-slice computed tomography. *Surg. Radiol. Anat.*, 41, 721–730. DOI: 10.1007/s00276-019-02210-1.

Ponzini R., Vergara C., Rizzo G., Veneziani A., Roghi A., Vanzulli A., Parodi O., Redaelli A., 2010. Womersley number-based estimates of blood flow rate in Doppler analysis: in vivo validation by means of phase-contrast MRI. *IEEE Trans. Biomed. Eng.*, 57, 1807–1815. DOI: 10.1109/TBME.2010.2046484.

Praharaj P., Sonawane C.R., Bongale A., 2024. Advancement in CFD and responsive AI to examine cardiovascular pulsatile flow in arteries: A Review. *Comput. Model. Eng. Sci.*, 141, 2021–2064. DOI: 10.32604/cmes.2024.056289.

Rahma A.G., Yousef K., Abdelhamid T., 2022. Blood flow CFD simulation on a cerebral artery of a stroke patient. *SN Appl. Sci.*, 4, 261. DOI: 10.1007/s42452-022-05149-y.

Ratajska A., Gula G., Flaht-Zabost A., Czarnowska E., Ciszek B., Jankowska-Steifer E., Niderla-Bielinska J., Radomska-Lesniewska D., 2014. Comparative and developmental anatomy of cardiac lymphatics. *Sci. World J.*, 2014, 183170. DOI: 10.1155/2014/183170.

Rzepliński R., Tarka S., Tomaszewski M., Kucewicz M., Acewicz A., Małachowski J., Ciszek B., 2025. Narrowings of the deep cerebral perforating arteries ostia: geometry, structure, and clinical implications. *J. Stroke*, 27, 52–64. DOI: 10.5853/jos.2024.01655.

Saaid H., Voorneveld J., Schinkel C., Westenberg J., Gijsen F., Segers P., Verdonck P., de Jong N., Bosch J.G., Kenjeres S., Claessens T., 2019. Tomographic PIV in a model of the left ventricle: 3D flow past biological and mechanical heart valves. *J. Biomech.*, 90, 40–49. DOI: 10.1016/j.jbiomech.2019.04.024.

Sadafi H., De Backer W., Krestin G., De Backer J., 2024. Rapid deposition analysis of inhaled aerosols in human airways. *Sci. Rep.*, 14, 24965. DOI: 10.1038/s41598-024-75578-9.

Salman H.E., Kamal R.Y., Yalcin H.C., 2021. Numerical investigation of the fetal left heart hemodynamics during gestational stages. *Front. Physiol.*, 12, 731428. DOI: 10.3389/fphys.2021.731428.

Samant S., Bakhos J.J., Wu W., Zhao S., Kassab G.S., Khan B., Panagopoulos A., Makadia J., Oguz U.M., Banga A., Fayaz M., Glass W., Chiastra C., Burzotta F., LaDisa J.F., Iaizzo P., Murasato Y., Dubini G., Migliavacca F., Mickley T., Bicek A., Fontana J., West N.E.J., Mortier P., Boyers P.J., Gold J.P., Anderson D.R., Tcheng J.E., Windle J.R., Samady H., Jaffer F.A., Desai N.R., Lansky A., Mena-Hurtado C., Abbott D., Brilakis E.S., Lassen J.F., Louvard Y., Stankovic G., Serruys P.W., Velazquez E., Elias P., Bhatt D.L., Dangas G., Chatzizisis Y.S., 2023. Artificial intelligence, computational simulations, and extended reality in cardiovascular interventions. *J. Am. Coll. Cardiol. Intv.*, 16, 2479–2497. DOI: 10.1016/J.JCIN.2023.07.022.

Sanz Sánchez J., Farjat Pasos J.I., Martinez Solé J., Hussain B., Kumar S., Garg M., Chiarito M., Teira Calderón A., Sorolla-Romero J.A., Echavarria Pinto M., Shin E.S., Diez Gil J.L., Waksman R., van de Hoef T.P., Garcia-Garcia H.M., 2023. Fractional flow reserve use in coronary artery revascularization: A systematic review and meta-analysis. *iScience*, 26, 107245. DOI: 10.1016/J.ISCI.2023.107245.

Schewe R.E., Khanafer K.M., Orizondo R.A., Cook K.E., 2012. Thoracic artificial lung impedance studies using computational fluid dynamics and in vitro models. *Ann. Biomed. Eng.*, 40, 628–636. DOI: 10.1007/s10439-011-0435-x.

Shang Y., Dong J., Tian L., Inthavong K., Tu J., 2019. Detailed computational analysis of flow dynamics in an extended respiratory airway model. *Clin. Biomech.*, 61, 105–111. DOI: 10.1016/j.clinbiomech.2018.12.006.

Shiina Y., Itatani K., Inai K., Niwa K., 2024. Energy loss and adults with congenital heart disease: a novel marker of cardiac workload beyond right ventricular size. *Cardiovasc. Diagn. Ther.*, 14, 1202–1209. DOI: 10.21037/cdt-24-296.

Skadorwa T., Eibl M., Zygańska E., Ciszek B., 2010. Radiological anatomy of the ambient cistern in children. *Folia Morphol.*, 69, 78–83.

Song M.-H., Sato M., Ueda Y., 2000. Three-dimensional simulation of coronary artery bypass grafting with the use of computational fluid dynamics. *Surg. Today*, 30, 993–998. DOI: 10.1007/s005950070019.

Standring S., Ellis H., Healy J., Johnson D., Williams A., Collins P., Wigley C., 2005. Gray's anatomy, 39th Edition: The anatomical basis of clinical practice. *Am. J. Neuroradiol.*, 26, 2703–2704.

Starling M.S., Kehoe L., Burnett B.K., Green P., Venkatakrishnan K., Madabushi R., 2024. The potential of disease progression modeling to advance clinical development and decision making. *Clin. Pharmacol. Ther.*, 117, 343–352. DOI: 10.1002/cpt.3467.

Sul B., Oppito Z., Jayasekera S., Vanger B., Zeller A., Morris M., Ruppert K., Altes T., Rakesh V., Day S., Robinson R., Reifman J., Wallqvist A., 2018. Assessing airflow sensitivity to healthy and diseased lung conditions in a computational fluid dynamics model validated in vitro. *J. Biomech. Eng.*, 140, 051009. DOI: 10.1115/1.4038896.

Syed F., Khan S., Toma M., 2023. Modeling dynamics of the cardiovascular system using fluid-structure interaction methods. *Biology*, 12, 1026. DOI: 10.3390/biology12071026.

Taylor C.A., Fonte T.A., Min J.K., 2013. Computational fluid dynamics applied to cardiac computed tomography for noninvasive quantification of fractional flow reserve: Scientific basis. *J. Am. Coll. Cardiol.*, 61, 2233–2241. DOI: 10.1016/j.jacc.2012.11.083.

Tebaldi M., Campo G., Biscaglia S., 2015. Fractional flow reserve: Current applications and overview of the available data. *World J. Clin. Cases*, 3, 678–681. DOI: 10.12998/wjcc.v3.i8.678.

Tomaszewski M., Kucewicz M., Rzepliński R., Małachowski J., Ciszek B., 2024. Numerical aspects of modeling flow through the cerebral artery system with multiple small perforators. *Biocybern. Biomed. Eng.*, 44, 341–357. DOI: 10.1016/j.bbe.2024.04.002.

Tsega E.G., 2018. Computational fluid dynamics modeling of respiratory airflow in tracheobronchial airways of infant, child, and adult. *Comput. Math. Methods Med.*, 2018, 9603451. DOI: 10.1155/2018/9603451.

Tsubata H., Nakanishi N., Itatani K., Takigami M., Matsubara Y., Ogo T., Fukuda T., Matsuda H., Matoba S., 2023. Pulmonary artery blood flow dynamics in chronic thromboembolic pulmonary hypertension. *Sci. Rep.*, 13, 6490. DOI: 10.1038/s41598-023-33727-6.

Tsuchiwata S., Tsuji Y., 2023. Computational design of clinical trials using a combination of simulation and the genetic algorithm. *CPT: Pharmacometrics Syst. Pharmacol.*, 12, 522–531. DOI: 10.1002/psp4.12944.

Tullio M., Aliboni L., Pennati F., Carrinola R., Palleschi A., Aliverti A., 2021. Computational fluid dynamics of the airways after left-upper pulmonary lobectomy: A case study. *Int. J. Numer. Method. Biomed. Eng.*, 37, e3462. DOI: 10.1002/cnm.3462.

Viola F., Del Corso G., De Paulis R., Verzicco R., 2023. GPU accelerated digital twins of the human heart open new routes for cardiovascular research. *Sci. Rep.*, 13, 8230. DOI: 10.1038/s41598-023-34098-8.

Wall W.A., Rabczuk T., 2008. Fluid–structure interaction in lower airways of CT-based lung geometries. *Int. J. Numer. Methods Fluids*, 57, 653–675. DOI: 10.1002/fld.1763.

Wang X., Li X., 2011. Computational simulation of aortic aneurysm using FSI method: Influence of blood viscosity on aneurismal dynamic behaviors. *Comput. Biol. Med.,* 41, 812–821. DOI: 10.1016/j.compbiomed.2011.06.017.

Wiśniewski K., Reorowicz P., Tyfa Z., Price B., Jian A., Fahlström A., Obidowski D., Jaskólski D.J., Jóźwik K., Drummond K., Wessels L., Vajkoczy P., Adamides A.A., 2024. Computational fluid dynamics; a new diagnostic tool in giant intracerebral aneurysm treatment. *Comput. Biol. Med.*, 181, 109053. DOI: 10.1016/j.compbiomed.2024.109053.

Wojtas K., Kozłowski M., Orciuch W., Makowski Ł., 2021. Computational fluid dynamics simulations of mitral Paravalvular leaks in human heart. *Materials*, 14, 7354. DOI: 10.3390/ma14237354.

Xi J., Kim J., Si X.A., Corley R.A., Kabilan S., Wang S., 2015. CFD modeling and image analysis of exhaled aerosols due to a growing bronchial tumor: Towards non-invasive diagnosis and treatment of respiratory obstructive diseases. *Theranostics*, 5, 443–455. DOI: 10.7150/thno.11107.

Xu X.Y., Ni S.J., Fu M., Zheng X., Luo N., Weng W.G., 2017. Numerical investigation of airflow, heat transfer and particle deposition for oral breathing in a realistic human upper airway model. *J. Therm. Biol.*, 70, 53–63. DOI: 10.1016/j.jtherbio.2017.05.003.

Yan Q., Xiao D., Jia Y., Ai D., Fan J., Song H., Xu C., Wang Y., Yang J., 2024. A multi-dimensional CFD framework for fast patient-specific fractional flow reserve prediction. *Comput. Biol. Med.*, 168, 107718. DOI: 10.1016/j.compbiomed.2023.107718.

Yang J., Zhang Y., Xue J., Guo Y., Liu S., Yao Y., Zhong H., Quan A., Yang J., 2025. Hemodynamic effects of stenosis with varying severity in different segments of the carotid artery using computational fluid dynamics. *Sci. Rep.*, 15, 4896. DOI: 10.1038/s41598-025-89100-2.

Zhang Z., Zhou X., Suarez-Pierre A., Lui C., Kearney S., Yeung E., Halperin H., Choi C.W., Katz J., 2020. Time-resolved echo-particle image/tracking velocimetry measurement of interactions between native cardiac output and veno-arterial ECMO flows. *J. Biomech. Eng.*, 143, 021008. DOI: 10.1115/1.4048424.

Zhu Y., Xu X.Y., Rosendahl U., Pepper J., Mirsadraee S., 2022. Prediction of aortic dilatation in surgically repaired type A dissection: A longitudinal study using computational fluid dynamics. *JTCVS Open*, 9, 11–27. DOI: 10.1016/J.XJON.2022.01.019.

Zhu Y., Xu X.Y., Rosendahl U., Pepper J., Mirsadraee S., 2023. Advanced risk prediction for aortic dissection patients using imaging-based computational flow analysis. *Clin. Radiol.*, 78, e155–e165. DOI: 10.1016/J.CRAD.2022.12.001.

Zobaer T., Sutradhar A., 2021. Modeling the effect of tumor compression on airflow dynamics in trachea using contact simulation and CFD analysis. *Comput. Biol. Med.*, 135, 104574. DOI: 10.1016/j.compbiomed.2021.104574.

Zuo X., Xu Z., Jia H., Mu Y., Zhang M., Yuan M., Wu C., 2022. Co-simulation of hypertensive left ventricle based on computational fluid dynamics and a closed-loop network model. *Comput. Methods Programs Biomed.*, 216, 106649. DOI: 10.1016/j.cmpb.2022.106649.

Chemical Engineering Horizons and Perspectives.
Article series endorsed by the Scientific Committee on Chemical and Process Engineering
of the Polish Academy of Sciences, term 2024–2027